

Gesture-Based Robot Control with Variable Autonomy from the JPL BioSleeve

Michael T. Wolf, Christopher Assad, Matthew T. Vernacchia, Joshua Fromm, and Henna L. Jethani

Abstract—This paper presents a new gesture-based human interface for natural robot control. Detailed activity of the user’s hand and arm is acquired via a novel device, called the BioSleeve, which packages dry-contact surface electromyography (EMG) and an inertial measurement unit (IMU) into a sleeve worn on the forearm. The BioSleeve’s accompanying algorithms can reliably decode as many as sixteen discrete hand gestures and estimate the continuous orientation of the forearm. These gestures and positions are mapped to robot commands that, to varying degrees, integrate with the robot’s perception of its environment and its ability to complete tasks autonomously. This flexible approach enables, for example, supervisory point-to-goal commands, virtual joystick for guarded teleoperation, and high degree of freedom mimicked manipulation, all from a single device. The BioSleeve is meant for portable field use; unlike other gesture recognition systems, use of the BioSleeve for robot control is invariant to lighting conditions, occlusions, and the human–robot spatial relationship and does not encumber the user’s hands. The BioSleeve control approach has been implemented on three robot types, and we present proof-of-principle demonstrations with mobile ground robots, manipulation robots, and prosthetic hands.

I. INTRODUCTION

The methods commonly used for humans to direct the actions of robots are cumbersome and insufficient for complex tasks. There is growing interest in using hand and arm gestures to supervise robots in environments shared with humans, with the aim of natural, intuitive, and flexible control interfaces. This paper presents our methods for gesture-based robot control, including integrating with various robot autonomy capabilities, using a novel wearable device, called the JPL BioSleeve.

The JPL BioSleeve (Fig. 1) incorporates sixteen surface electromyography (EMG) channels and an inertial measurement unit (IMU) into an easily donned, low profile package worn on the user’s forearm. By monitoring the forearm muscles, the BioSleeve can achieve detailed tracking of the fingers and hand without requiring hand-worn equipment, while the IMU provides information on arm motion and position [1]. The aim of the BioSleeve is to develop a portable, robust system to control highly capable robots in

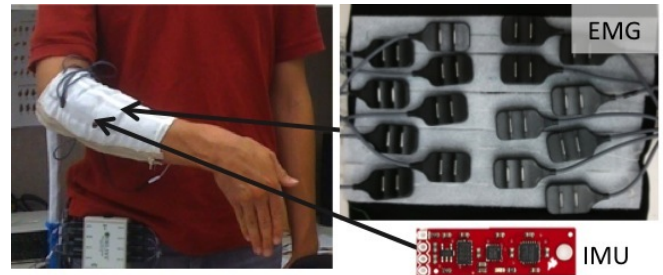


Fig. 1. The JPL BioSleeve. The BioSleeve has 16 dry contact EMG sensors and a small IMU with magnetometer. The elastic sleeve has a zipper closure and hook-and-loop fasteners on the inside to allow rearrangement of electrodes. Note there is no need for precision alignment of sensors.

the human’s environment, for applications such as an astronaut commanding construction robots on the moon, operators of urban search and rescue robots, or soldiers commanding bomb disposal or scout robots. Further, since the muscles that actuate the hand often remain intact after a transradial amputation, the BioSleeve may also have applications for controlling actuated hand prostheses.

The variable autonomy of our approach aims to maximize the user’s control while minimizing the required input and user attention. Supervised autonomy commands are key to leveraging the robot’s own capabilities to reduce operator burden. However, operators will sometimes require more precise authority over the robot. Thus, flexibility is an important component for control interfaces—we present command modes for point-to-goal operations, stored procedures, virtual joysticking / guarded teleoperation, mimicked manipulation, and command set switching / robot selection. For goal-based commands, we utilize not only the robots motion autonomy for executing the command but also its perception autonomy for disambiguating the user’s intent.

Current research in gesture-based interfaces typically relies on computer vision for observing and classifying the human gestures (see [2] for a survey), and numerous researchers have investigated using visually identified gestures for commanding robots [3]–[8], including point-to-object operations [9], [10]. Compared to using the BioSleeve, vision-based approaches have the advantage of avoiding human-worn equipment. However, cameras work best only in controlled environments, often requiring constant camera–human spatial relationships and consistent lighting [2]. For our applications, visual systems generally lack the robustness required for mobile, outdoor field use—which may entail arbitrary changes in perspective, highly variable lighting conditions, occlusions between the human and camera, and large distances between the human and robot.

This research was conducted at the Jet Propulsion Laboratory, California Institute of Technology, under a contract with the National Aeronautics and Space Administration.

M. T. Wolf and C. Assad are with the Jet Propulsion Laboratory, California Institute of Technology, Pasadena, CA 91109 USA. (e-mail: wolf@jpl.nasa.gov)

M. T. Vernacchia and H. L. Jethani are students in the Department of Aeronautics and Astronautics at the Massachusetts Institute of Technology.

J. Fromm is a student in the Division of Engineering and Applied Sciences at the California Institute of Technology.

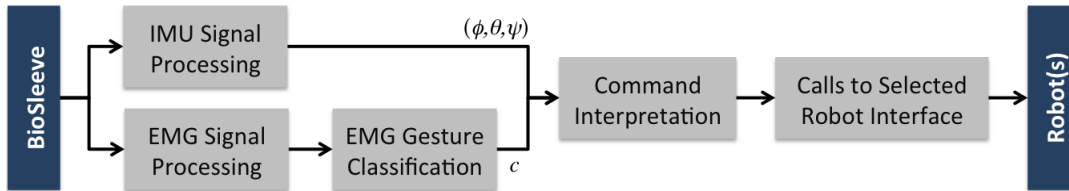


Fig. 2. Functional data flow from BioSleeve signals to robot commands. The IMU and EMG signals are first processed independently; then the resulting hand gesture class and the arm orientation are used jointly for command interpretation.

Another approach for gesture recognition is to use inertial sensors to estimate the human’s body posture [11]–[13]. We similarly use inertial sensing for gross posture information, but detailed information about hand/finger positions is not available in the above works. Some glove-based inertial sensor systems estimate hand and finger position, but having the hands covered in sensor gloves is at the least cumbersome and sometimes impracticable for field users, such as when carrying equipment or completing manipulation tasks. Besides leaving the hands free, the BioSleeve EMG sensors provide data regarding not only the hand/finger positions but also the muscle *forces*, information we use in our robot control paradigm but unavailable to inertial or visual sensors.

Forearm EMG has been previously shown to provide accurate representations of hand movement [14], and EMG signals have been used in limited ways for robot control, without autonomy integration. Wheeler et al. demonstrated virtual joystick commands for a human–computer interface [15]. Kim et al. controlled an RC car with four commands from a single electrode [16]. Artemiadis et al. used EMG for gross arm (not hand) position for reflected motion of a robot arm [17]. Our work differs in that we integrate both EMG and IMU signals, decode a significantly larger number of gestures, and demonstrate several different types of commands (levels of autonomy). Also, we show coordination with the robots’ autonomy systems (for both perception and motion) to ease the operational burden, and use the muscle force as a variable parameter to aid in precision control.

An overview of our approach is illustrated in Fig. 2. The BioSleeve hardware, described in Sect. II, collects EMG and IMU signals. These signals are first processed independently, using a classification algorithm to decode the hand position from the EMG signals, as summarized in Sect. III. This output is then used by the command interpretation algorithms (Sect. IV) to map gestures into variable autonomy robot commands. Results of using the BioSleeve to control three different robot types are presented in Section V.

II. THE JPL BIOSLEEVE

The BioSleeve is designed to enable detailed, high degree-of-freedom (DOF) arm and hand tracking by integrating: (1) an array of dry-contact active EMG sensors to monitor muscle activations in the arm, (2) IMU sensor(s) to estimate limb orientation with respect to the body, and (3) in-sleeve processing for gesture recognition.

The current BioSleeve prototype is shown in Fig. 1. It incorporates sixteen commercial dry-contact surface EMG sensors (Delsys, Inc.), which have active bipolar channels.

The sensor array is positioned on the proximal forearm near the elbow, to monitor activation of the major forearm muscles. These EMG signals contain a combination of force and position information for the wrist and fingers. We packaged the sensors in a tight-fitting elastic sleeve to provide constant mechanical pressure and maintain good skin contact.

To complement the EMG sensor array, a small IMU “sensor stick” (Sparkfun Electronics) is also mounted on the BioSleeve to monitor forearm motion. Optionally, an additional IMU is strapped to the upper arm for full arm monitoring. The IMUs fuse data from a 3-axis gyroscope, 3-axis accelerometer, and 3-axis magnetometer. Such data enables model-constrained pose estimation of the limb segments (e.g., see [11]). Combined with the EMG array, IMU sensors can provide sufficient information to distinguish gestures from a large set of high DOF arm and hand motions.

The current BioSleeve prototype transmits raw sensor data over a tether to an off-board computer for processing. (We plan to implement the gesture recognition algorithms with in-sleeve processing, to minimize the bandwidth required to communicate gestures to a remote receiver.) Our long-term goal is to design a wireless, fully enclosed BioSleeve system with the following properties: (a) Ease-of-use: The BioSleeve will be conveniently embedded into wearable garments, donned and doffed as part of daily clothes. No extra setup time is required for placement of individual electrodes, fine alignment, etc. (b) Free mobility: There are no external sensors, hand obstructions, or electrode wires imposing constraints on allowable movements. (c) Reliability: Large dense sensor arrays add redundancy and are more immune from movement artifacts (electrode slippage, etc.), with the potential to dramatically improve decoding reliability. (d) Durability: Active channel selection and low power consumption per channel enables operation for long periods of time on in-sleeve batteries. (e) Versatility: The output of the gesture recognition can be mapped into various command libraries for different robotic systems, such as those detailed below. The research presented here describes intermediate steps to demonstrate the viability of the BioSleeve approach to robot control.

III. SIGNAL PROCESSING AND CLASSIFICATION

The arm and hand position of the user are decoded from the raw EMG and IMU signals, so they can be mapped to robot commands. The BioSleeve IMU provides the user’s gross forearm position. Also, for the mimicked manipulation commands (Sect IV-A), an additional IMU is strapped to the user’s upper arm for full arm pose. Our applications only

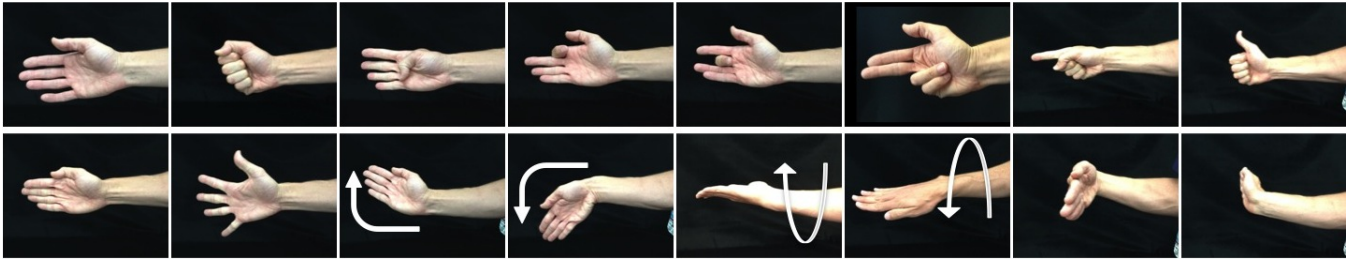


Fig. 3. Example gesture library. This gesture library has 16 hand gestures corresponding to various finger and wrist positions.

require the instantaneous angles of the user’s arm linkages, which are calculated in vendor-provided firmware for each IMU. These angles are denoted by $\mathbf{a}_l^k = (\phi_l^k, \theta_l^k, \psi_l^k)^T$, the roll, pitch, and yaw, respectively, for time step k , where $l = 1$ for the forearm and $l = 2$ for the upper arm.

The methods for decoding the wrist and finger positions from the forearm muscle activity read by surface EMG are summarized below. The raw electrode signals are amplified and band-pass filtered, then analyzed in 500-ms windows at a rate of 10 Hz (i.e. there is an overlap of 400 ms between adjacent time windows). Within the k th time window, we extract the feature vector $\mathbf{x}^k = (x_1^k, \dots, x_d^k)^T$, where x_j^k is the standard deviation of the signal for the j th electrode, $j = 1, \dots, d$. We find the standard deviation provides a good measure of muscle activity, as it is correlated to the signal amplitude but invariant to offsets.

We classify the feature vector \mathbf{x}^k using a multi-class support vector machine classifier (SVM) with radius basis function kernel [18], [19]. After donning the BioSleeve, the user is instructed to hold each of the N gestures for a brief period (typically 6 seconds). The labeled features collected in this session are used to train the SVM, after which each incoming \mathbf{x}^k is classified in real time as one of the gestures, $c^k \in \mathcal{C} = \{c_1, \dots, c_N\}$ (see Fig. 3 for an example set with 16 gestures). We achieved classification accuracies of 96% for a 16-gesture dataset. In most cases, a user only needs four to six gestures to perform a robot control task, for which classification usually exceeds 99%. (See [1] for further information on EMG decoding algorithms and performance.) Further, if we wish to expand the space of classified gestures, we can easily augment the input space with the IMU data and define a gesture based not only from EMG class but also from the forearm pitch angle—i.e., use $\{c^k, \theta_1^k \in \Theta\}$ for classification, where Θ defines a discretization of the pitch angle (e.g., discretizing into five angle bins increases the number of gestures detected by five-fold).

IV. INTERPRETATION OF ROBOT COMMANDS

This section describes how we use the classified hand gesture c^k and arm linkage orientations $\{\mathbf{a}_l^k\}$ to define robot commands. Here, we group these commands into “types” that define soft categories of how the commands are used and the level of corresponding robot autonomy required; types are defined more for the user’s mental control model rather than for technical implementation. While further user studies are required to define the best commands for a given

application, the types and commands below were chosen to investigate the broad usefulness of a BioSleeve-based interface over various levels of autonomy. Some command types utilize the high-DOF input of the BioSleeve for direct teleoperation, while others focus on the ability to send supervisory commands using simple gestures.

A. Mimicked Manipulation (\mathcal{T}_{MM})

Mimicked manipulation commands (i.e., commands of type \mathcal{T}_{MM}), enable the user to operate a robot manipulator by example—the robot directly imitates the high-DOF motions of the user, typically without any reliance on autonomy. To control motions of a robotic hand, for example, our system maps gesture classes c^k to corresponding robot finger and wrist positions. This type of hand control applies perhaps most commonly to anthropomorphic hands but is also useful on arbitrary robotic grippers.

\mathcal{T}_{MM} commands also enable direct position control of the robot end effector simply by moving the user’s hand as desired. In this case, we estimate the user hand position through human arm forward kinematics with joint angles given by $\{\mathbf{a}_1^k, \mathbf{a}_2^k\}$ and arm linkage lengths $L_1 = L_2 \equiv L$. We provide a user parameter α to scale the user’s hand movements to the robot’s, such that the robot end effector position is calculated with linkage length $\tilde{L} = \alpha L$. Note, however, that we have chosen to control only the end effector position, not to specify the robot arm configuration—this enables use with robot arms with arbitrary kinematics rather than limiting to those with kinematics similar to the human’s.

B. Virtual Joystick (\mathcal{T}_{VJ})

The virtual joystick commands, type \mathcal{T}_{VJ} , provides direct operation applicable to controlling the velocity of ground robots. We have specifically implemented commands for forward and backward motion and left and right in-place turns using wrist positions. A novel technique we have developed for this mode is a variable speed control. As noted earlier, an advantage of using EMG is that it measures muscle forces; the 2-norm $\rho^k = \|\mathbf{x}^k\|$ provides an indication of the force with which the user holds the gesture. (Typically, the distribution of the M samples $\{\mathbf{x}^k\}_{k=1}^M$ within a given class’s training data is approximately Gaussian with a principal axis nearly intersecting the origin, indicating that force is the largest source of in-class variability.) For each class, we find ρ_{\min} and ρ_{\max} , the minimum and maximum values, respectively, of the set of training sample norms. To set the speed, v^k , of the movement command c^k , we interpolate

between maximum and minimum values of vehicle (linear or angular) speeds, v_{\min} and v_{\max} , given the incoming command c^k with feature norm ρ^k :

$$v^k = \begin{cases} \frac{v_{\max} - v_{\min}}{\rho_{\max} - \rho_{\min}} \rho^k & \rho^k \in [\rho_{\min}, \rho_{\max}] \\ v_{\min} & \rho^k < \rho_{\min} \\ v_{\max} & \rho^k > \rho_{\max}. \end{cases} \quad (1)$$

The resulting speed control allows the user an intuitive mechanism for trading between precision and completion time.

Robots executing \mathcal{T}_{VJ} commands employ a degree of robot autonomy if the commands are set to operate in a “guarded teleoperation” mode. In this mode, the robot uses its own sensor data as a safety check on the user commands, to stop motion if the command involves, for example, a collision or falling off a ledge.

C. Stored Procedures (\mathcal{T}_{SP})

Gestures may also be used to initiate a pre-programmed set of instructions (a stored procedure) for the robot to execute. While these commands of type \mathcal{T}_{SP} are operationally simple, requiring only a simple one-time trigger, they serve as an example of the convenience of using autonomy instead of demanding the user’s continuous attention. For example, a robot may be given a brief command to “navigate straight ahead, avoiding obstacles”, “make a U-turn”, “return the manipulator arm to home position”, etc., instead of teleoperating the robot through these motions. Often, \mathcal{T}_{SP} commands are used in conjunction with commands of other types, with switching based on α_i^k . For instance, flexion of the right wrist (gesture c_{15}) is often used to indicate “turn left”—but the user can change his/her arm angle from horizontal to vertical to switch whether this should be done as a virtual joystick or stored procedure command:

$$\begin{aligned} \{c^k = c_{15}, \theta_1^k > -60^\circ\} &\Rightarrow \text{continuous left turn } (\mathcal{T}_{VJ}) \\ \{c^k = c_{15}, \theta_1^k \leq -60^\circ\} &\Rightarrow 90^\circ \text{ left turn } (\mathcal{T}_{SP}). \end{aligned} \quad (2)$$

D. Point-to-Goal (\mathcal{T}_{PG})

Users can indicate navigation/manipulation goals by pointing, a powerful use of the BioSleeve since it enables the user to mentally operate in his own frame of reference and utilizes a high degree of autonomy to specify and complete the task. When the user makes the pointing gesture (c_7), we capture the pointing angle α_1^k . We then define a *pointing ray*, $(\mathbf{x}_h^k, \hat{\mathbf{u}}_h^k)$, originating at the user’s shoulder position, \mathbf{x}_h^k with direction defined by unit vector $\hat{\mathbf{u}}_h^k$, which is derived from the pitch, θ_1^k , and yaw, ψ_1^k , of the user’s forearm. (In this work, we have assumed the user’s approximate shoulder position relative to the robot is known via GPS or other means. Although this is a strong assumption, robust and precise localization for humans, robots, and mixed teams is an active and promising area of research.)

For manipulator arms, we have applied \mathcal{T}_{PG} commands to indicate which objects the robot should grasp and pick up. In our implementation, the robot’s perception system has identified, say, n objects in its environment; let \mathbf{y}_j be the

position of the j th object in the user body frame (centered at \mathbf{x}_h^k). Then, an object is selected according to its cosine similarity with the pointing vector:

$$f(j) = \frac{\mathbf{y}_j - \mathbf{x}_h^k}{\|\mathbf{y}_j - \mathbf{x}_h^k\|} \cdot \hat{\mathbf{u}}_h^k, \quad j = 1, \dots, n \quad (3)$$

$$j^* = \arg \max_j f(j). \quad (4)$$

The object j^* is passed to the robot as the manipulation goal if it passes the test

$$f(j^*) > \cos \gamma, \quad (5)$$

where γ is the threshold for maximum allowable angle between the pointing ray and the ray towards the object.

For mobile robots, \mathcal{T}_{PG} commands have been used to indicate ground positions to which the robot should navigate. To accomplish this, we find the intersection of the ray $(\mathbf{x}_h^k, \hat{\mathbf{u}}_h^k)$ and the ground plane, resulting in the goal location \mathbf{x}_g . The robot is then sent a command to go to \mathbf{x}_g autonomously, so it can use its own sensor feedback and navigation capabilities to execute a safe, feasible path.

E. Switching Between Command Sets and Robots (\mathcal{T}_{CS})

A *command set* defines an application-oriented mapping between gesture input $\{c^k, \alpha_1^k\}$ and the commands sent to a particular robot. The purpose of having multiple command sets is twofold: to provide a very large library of user commands using a hierarchical strategy (increasing accuracy and decreasing the mental load on the user), and to switch between which robot (or which subsystem of a given robot, e.g., mobility vs. manipulation) is being controlled. \mathcal{T}_{CS} gestures enable the user to switch between these command sets, including the ability to switch between which robots. In our implementations, we have typically reserved gestures with the user’s forearm being held vertically upward to indicate \mathcal{T}_{CS} commands:

$$\begin{aligned} \{c^k = c_{s_1}, \theta_1^k > 60^\circ\} &\Rightarrow \text{command set 1} \\ &\vdots \\ \{c^k = c_{s_n}, \theta_1^k > 60^\circ\} &\Rightarrow \text{command set n} \end{aligned} \quad (6)$$

We have found this strategy provides the user a great deal of flexibility for the user without disrupting normal operation.

V. RESULTS

We have implemented BioSleeve gesture control for three robotic platforms: a manipulation system, a small ground robot, and a five-fingered hand. Specific demonstrations are described below as well as presented in an accompanying video. The goal of this work was to demonstrate proof of principle that a BioSleeve-like system can provide a reliable, flexible method for robot control, rather than accomplish a quantitative user study. (Indeed, largely because our aim is to show the approach’s flexibility and variable autonomy in applications not appropriate for visual, manipulandum, or glove-based systems, it is yet unclear what systems should be quantitatively compared.) Table I lists commands used for

each robot; the list is not exhaustive but provides a spectrum of relevant command types. In all command sets, the “rest” position (c_1) is mapped to “no command”.

TABLE I
EXAMPLE COMMANDS IMPLEMENTED FOR EACH ROBOT TYPE

Robot	Command	Type
Manipulator Arm	Pick up object	\mathcal{T}_{PG}
	Move end effector	\mathcal{T}_{MM}
	Open gripper	\mathcal{T}_{MM}
	Close gripper	\mathcal{T}_{MM}
	Scan the environment	\mathcal{T}_{SP}
	Put down object	\mathcal{T}_{SP}
	Grasp type A	\mathcal{T}_{SP}
	Grasp type B	\mathcal{T}_{SP}
Ground Robot	Move to goal	\mathcal{T}_{PG}
	Forward	\mathcal{T}_{VJ}
	Backward	\mathcal{T}_{VJ}
	Left	\mathcal{T}_{VJ}
	Right	\mathcal{T}_{VJ}
	U-turn	\mathcal{T}_{SP}
	90° left	\mathcal{T}_{SP}
	90° right	\mathcal{T}_{SP}
	Dance	\mathcal{T}_{SP}
	Select robot 1	\mathcal{T}_{CS}
	Select robot 2	\mathcal{T}_{CS}
	Hand	Close finger 1
Close finger 2		\mathcal{T}_{MM}
Close finger 3		\mathcal{T}_{MM}
Close fingers 4–5		\mathcal{T}_{MM}
Close fingers 1–5		\mathcal{T}_{MM}
Open all fingers		\mathcal{T}_{MM}



Fig. 4. Point-to-goal command to the manipulation robot: The user points to the impact driver of the left part of the table.

The manipulation robot (used for the DARPA Autonomous Robotic Manipulation (ARM) program) is equipped with two Barrett WAM arms, each with a BarrettHand (Barrett Technology, Inc.) and stereo vision and other sensors. For tests of supervisory commands, three objects were placed on a table in front of the robot, and the user stood outside of the field of view of the robot (see Fig. 4). The user instructed the robot to scan the table for objects, after which the user pointed to an object to instruct the robot to pick it up, which the robot did autonomously. The user then instructed the robot to place the object back down on the table. In a mimicked manipulation mode, the user could move his hand to place the robot end effector at a desired location; also, hand gestures were mapped to open and close the gripper and change the finger configuration from opposed (grasp type “A”) or together (grasp type “B”). Gesture recognition during these tests had extremely high accuracy. Indicating goals by pointing also worked very well but had occasional

false associations when objects were closely spaced—these errors were tracked to a drifting yaw angle, which might be caused by magnetic interference in the basement laboratory where the tests were conducted.

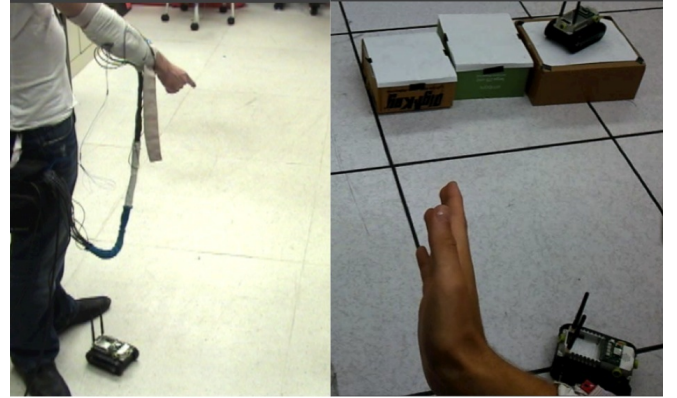


Fig. 5. Commands to the ground robot: (left) the user points to a ground position as the navigation target; (right) a virtual joystick command for the vehicle to turn right

For ground robot operation, we sent commands to the small tracked LANDroid robots (iRobot Corp.); see Fig. 5. \mathcal{T}_{PG} commands were initiated by pointing to goal locations on the floor. The point-to-goal results successfully demonstrated proof of principle as desired, though the LANDroid navigated only by track odometry, which caused (growing) errors in the actual position achieved by the robot. Tests of driving the robot by virtual joystick and stored procedures included (a) routing the robot through a short obstacle course and (b) using two robots in a cooperative task to get robot A across a “bridge” completed by robot B (see accompanying video). In the latter scenario, the user switched between which robot was “selected” using \mathcal{T}_{CS} commands. When driving through the obstacle course, \mathcal{T}_{VJ} commands were enabled with the guarded teleoperation mode, in which the robot would use its IR proximity sensors to stop, overriding the user command to avoid collisions.

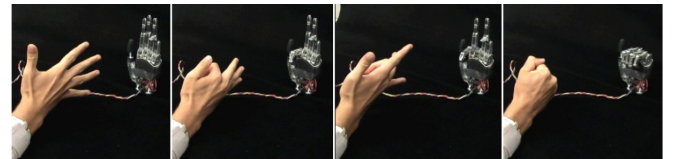


Fig. 6. Commands being sent to the actuated hand: (left to right) open fingers, close index finger, close middle finger, close all fingers

The actuated hand (Harada Electric Industry, Inc.) provided a testbed for end effectors more anthropomorphic than the BarrettHand and a surrogate for prosthesis control. This platform has no sensing or autonomy, and \mathcal{T}_{MM} commands were simply mapped to motor controls (1 DOF per finger). These tests showed that individual finger movements can be controlled by the BioSleeve system, as shown in Fig. 6. Note that individual motion of the fourth and fifth fingers are difficult to distinguish, and rarely employed in common practice; therefore, these fingers were grouped together for classification and control.

The video that accompanies this paper shows the following examples of live operation for the three systems:

- 1) Manipulation arm: Opening and closing the hand; picking up objects from the table from pointing commands; placing object on the table.
- 2) Ground robot: Point to navigation goal; virtual joystick driving with robot switching; stored procedure.
- 3) Hand: Moving individual fingers; making fist; opening hand.

VI. CONCLUSION

We have presented a novel system that enables humans to send commands to robots using gestures and have demonstrated the versatility of the system to provide many types of commands to several robot platforms. By capturing EMG and IMU signals from our forearm-worn BioSleeve, we are able to extract accurate information about the detailed hand position and gross arm position, without the limitations of vision systems and without requiring hand-worn equipment.

Integrating commands with the robot's own autonomous capabilities makes the system easier to use and safer than operating with only human input, and our system has the flexibility of initiating commands at variable autonomy levels. In point-to-goal commands, we enable the user to naturally operate in his own reference frame and integrate with the robot's perception system to help disambiguate the goal—or operate in a continuous space to indicate arbitrary navigation goals. For virtual joystick commands, we not only send direction commands but also leverage the muscle forces read by the EMG signal to modulate the robot's speed. Mimicked manipulation commands make use of the BioSleeve's ability to capture detailed finger positioning and naturally control many DOFs.

While we have demonstrated the prototype system for several scenarios, many items remain for future work, including: using dynamic gestures to direct robots; implementing different styles of pointing gestures to indicate different types of objects/cues; establishing a robot–user dialogue to provide salient information feedback to the user about the robot's planned action; constructing a truly wireless device with processing fully embedded in the BioSleeve; and integrating with localization algorithms for full mobility of the human in point-to-goal operations. Additionally, we plan further user studies and comparative quantitative performance analysis with other possible systems, as well as analysis of long-term performance of the BioSleeve to understand if EMG electrical variations or slippage cause issues. Finally, we wish to combine the BioSleeve interface with other modalities, such as voice control, to enable further operational options and flexibility. In total, we aim that this technology provides the missing link for people to robustly supervise and direct robots in shared environments.

ACKNOWLEDGMENTS

Part of this work was sponsored by the Defense Advanced Research Projects Agency (DARPA) MTO under the auspices of Dr. Jack Judy through the Army Research Office,

Contract No. MIPR2C080XR010. We would also like to thank Dr. Nicolas Hudson and the JPL DARPA ARM team.

REFERENCES

- [1] M. T. Wolf, C. Assad, K. You, H. Jethani, M. Vernachia, J. Fromm, Y. Iwashita, and A. Stoica, "Decoding static and dynamic arm and hand gestures from the JPL BioSleeve," in *IEEE Aerospace Conference*, 2013.
- [2] S. Mitra and T. Acharya, "Gesture recognition: A survey," *Systems, Man, and Cybernetics, Part C: Applications and Reviews, IEEE Transactions on*, vol. 37, no. 3, pp. 311–324, May 2007.
- [3] D. Perzanowski, A. Schultz, and W. Adams, "Integrating natural language and gesture in a robotics domain," in *IEEE Int. Symp. Intelligent Control*, ser. ISIC '98, Sep. 1998, pp. 247–252.
- [4] S. Waldherr, R. Romero, and S. Thrun, "A gesture based interface for human-robot interaction," *Autonomous Robots*, vol. 9, pp. 151–173, 2000.
- [5] R. Stiefelwagen, C. Fugen, R. Gieselmann, H. Holzapfel, K. Nickel, and A. Waibel, "Natural human-robot interaction using speech, head pose and gestures," in *IEEE/RSJ Int. Conf. on Intelligent Robots and Systems (IROS)*, vol. 3, Sep. 2004, pp. 2422–2427.
- [6] H.-D. Yang, A.-Y. Park, and S.-W. Lee, "Gesture spotting and recognition for human-robot interaction," *IEEE Trans. Robotics*, April 2007.
- [7] B. Fransen, V. Morariu, E. Martinson, S. Blisard, M. Marge, S. Thomas, A. Schultz, and D. Perzanowski, "Using vision, acoustics, and natural language for disambiguation," in *ACM/IEEE Int. Conf. on Human-Robot Interaction*, ser. HRI '07. New York, NY, USA: ACM, 2007, pp. 73–80.
- [8] B. Burger, I. Ferrané, F. Lerasle, and G. Infantes, "Two-handed gesture recognition and fusion with speech to command a robot," *Autonomous Robots*, vol. 32, pp. 129–147, 2012.
- [9] A. G. Brooks and C. Breazeal, "Working with robots and objects: revisiting deictic reference for achieving spatial common ground," in *ACM SIGCHI/SIGART Conf. on Human-Robot Interaction*, ser. HRI '06. New York, NY, USA: ACM, 2006, pp. 297–304.
- [10] J. Schmidt, N. Hofemann, A. Haasch, J. Fritsch, and G. Sagerer, "Interacting with a mobile robot: Evaluating gestural object references," in *Intelligent Robots and Systems, 2008. IROS 2008. IEEE/RSJ International Conference on*, Sep. 2008, pp. 3804–3809.
- [11] E. Bachmann, X. Yun, and R. McGhee, "Sourceless tracking of human posture using small inertial/magnetic sensors," in *IEEE Int. Symp. on Computational Intelligence in Robotics and Automation*, vol. 2, Jul. 2003, pp. 822–829.
- [12] N. Miller, O. Jenkins, M. Kallmann, and M. Mataric, "Motion capture from inertial sensing for untethered humanoid teleoperation," in *IEEE/RAS Int. Conf. on Humanoid Robots*, vol. 2, nov. 2004, pp. 547–565.
- [13] H. Harms, O. Amft, G. Tröster, and D. Roggen, "SMASH: a distributed sensing and processing garment for the classification of upper body postures," in *Int. Conf. on Body Area Networks (BodyNets)*, 2008, pp. 22:1–22:8.
- [14] F. Tenore, A. Ramos, A. Fahmy, S. Acharya, R. Etienne-Cummings, and N. Thakor, "Decoding of individuated finger movements using surface electromyography," *IEEE Trans. Biomedical Eng.*, vol. 56, no. 5, pp. 1427–1434, May 2009.
- [15] K. Wheeler, M. Chang, and K. Knuth, "Gesture-based control and EMG decomposition," *IEEE Trans. Systems, Man, and Cybernetics, Part C: Applications and Reviews*, vol. 36, no. 4, pp. 503–514, Jul. 2006.
- [16] J. Kim, S. Mastnik, and E. André, "EMG-based hand gesture recognition for realtime biosignal interfacing," in *Proc. of the 13th Int. Conf. on Intelligent User Interfaces (IUI)*. New York, NY, USA: ACM, 2008, pp. 30–39.
- [17] P. Artemiadis and K. Kyriakopoulos, "EMG-based control of a robot arm using low-dimensional embeddings," *IEEE Trans. Robotics*, vol. 26, no. 2, pp. 393–398, Apr. 2010.
- [18] V. Vapnik, *Estimation of Dependences Based on Empirical Data*. Springer Verlag, 1982.
- [19] J. Shawe-Taylor and N. Cristianini, *Support Vector Machines and other kernel-based learning methods*. Cambridge University Press, 2000.